

Evolutionary properties of massive AGB stars

L. Siess¹ and M.L. Pumo²

¹ Institut d'Astronomie et d'Astrophysique Université Libre de Bruxelles - Boulevard du triomphe CP 226 - B-1050 Bruxelles - Belgium
e-mail: siess@astro.ulb.ac.be

² Università di Catania, Dip. di Fisica ed Astronomia (sez. Astrofisica), Città Universitaria, via S. Sofia N.78, I-95123 Catania, Italy

Abstract. We review the evolution of massive AGB stars, the so-called Super-AGB stars, that ignite carbon off-center but do not proceed through all nuclear burning stages. The mass range of these stars is confined to a narrow range, between 7 and 11 M_{\odot} depending on the metallicity. We also analyze the fate of these stars, neon-oxygen white dwarf or electron-capture supernova (EC-SN), as a function of metallicity. Our results indicate that the mass range for EC-SN is very narrow, of the order of 1 M_{\odot} . A brief overview of the characteristics of the thermally pulsing SAGB phase is finally presented.

Key words. Stars: AGB – Stars: evolution – Stars: nucleosynthesis

1. Introduction

Super-AGB (SAGB) stars have typical masses ranging between 7 and 11 M_{\odot} . This stellar population draws the bridge between on one side “standard” AGB stars that end their life as CO white dwarfs and on the other side massive stars that proceed through all nuclear burning stages and end-up as iron core collapse supernova. SAGB stars evolution is characterized by the off-center ignition of carbon in condition of partial degeneracy. The outcome of this evolution, primary depending on the mass loss rate and of the presence or not of third dredge up episodes, can either be a neon-oxygen (NeO) white dwarf or a neutron star as a result of electron captures induced core collapse (EC-SN).

According to the standard Salpeter IMF, SAGB stars are rather numerous (about 1/2 - 1/3 of all stars with $M \gtrsim 7M_{\odot}$) and undoubtedly must play a role in the chemical evolution of galaxy. However, large uncertainties still enshrouds their evolution and nucleosynthesis, and the lack of SAGB stars models prevent us from having an estimate for their yields.

In this paper, we present new results concerning their evolution (§2), fate (§3) and nucleosynthesis during the thermally pulsing AGB phase (§4). Based on these new results, we give in the last section some expectations concerning of their role in the chemical evolution of galaxies.

2. Structural Evolution

Prior to carbon ignition, the evolution of massive AGB stars is very similar to their lower

Send offprint requests to: L. Siess

mass counterpart. During the main sequence, the CNO cycle provides the nuclear energy production and a convective core maintains until central H exhaustion. Then the region of nuclear burning moves into a shell surrounding a contracting core. The large release of gravitational energy produces a substantial expansion of the radius and induces the deepening of the convective envelope. During the so-called first dredge-up, the convection zone penetrates into the regions of H burning and brings to the surface the ashes of the CNO cycle mainly, i.e. ^{14}N , ^{13}C and ^4He . As far as the chemical composition is concerned, in massive AGB stars the chemical signatures of the first dredge-up are almost indistinguishable from their lower mass counterpart, the most notorious difference being their higher luminosity.

As the envelope retreats, the temperature in the core reaches $\sim 10^8\text{K}$ and He ignites at the center. The steep temperature dependence of the 3α reactions leads to the formation of a convective core. The modeling of core He burning is a hard problem in stellar evolution calculations, in particular near the end of the phase when the core He mass fraction $Y \lesssim 0.1$. At this stage, because of the presence of semiconvective layers surrounding the core, the convective boundaries are very sensitive to any perturbations (numerical or physical, see e.g. Straniero *et al.* 1993). The determination of the He-depleted core mass reveals very code-dependent which is unfortunate since this value strongly influences the subsequent evolution of the star.

2.1. The carbon burning phase

At central He-exhaustion, core contraction resumes, the central density increases and plasma neutrino emission rises. Energy is efficiently removed from the core which cools down and becomes more and more degenerate. As a consequence, the location of the maximum temperature moves outward. In “standard” AGB stars, the increase in the peak temperature (T_{max}) ceases when the energy produced in H burning shell is able to balance the energy lost at the surface. Thereafter, owing to the shielding effect of the HBS, core con-

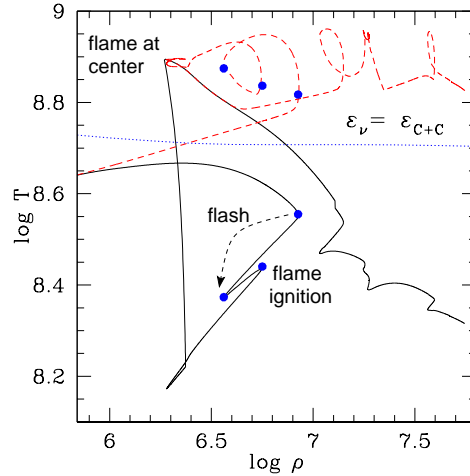


Fig. 1. Evolution of a representative $9.5M_{\odot}$, $Z = Z_{\odot}$ star in the $\rho_c - T_c$ plane. The dotted line indicates the locus where the neutrino energy loss rate (ϵ_{ν}) equals the nuclear energy production rate by carbon burning ($\epsilon_{\text{C+C}}$). The solid and dashed lines represent the run of the central and maximum temperature, respectively.

traction almost stops and the peak temperature slowly decreases from pulse to pulse. In massive AGB stars however, because of the larger core mass at the end of central He burning, the maximum temperature can cross the carbon ignition line defined in the $\rho_c - T_c$ plane by $\epsilon_{\nu} = \epsilon_{\text{C+C}}$ (Fig. 1).

Carbon burning then proceeds in two steps (e.g. Siess 2006a). First, the development of a violent carbon flash which induces a significant expansion of the core as can be seen in Fig. 1 from the decrease in both T_c and ρ_c . This structural readjustment quenches the convective instability which disappears after a few hundred years (Fig. 2). Core contraction then resumes until the maximum temperature reaches the deeper layers of the core where the fuel is abundant. At carbon re-ignition, a second convective zone develops. However in this case the released energy is considerably reduced because the flash has partially lifted the degeneracy at the ignition point and most importantly because the convective instability develops in the region previously occupied by the

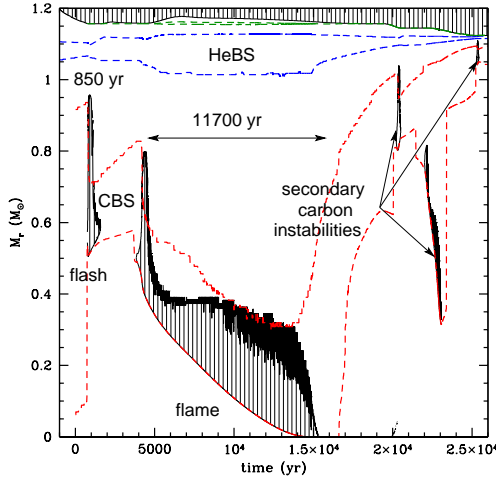


Fig. 2. Evolution of the internal structure of a $9.5M_{\odot}$, $Z = Z_{\odot}$ during the carbon burning phase.

flash. During the second convective episode the carbon luminosity $L_c \lesssim 10^6 L_{\odot}$, much smaller than the $10^7 L_{\odot}$ emitted during the flash of our $9.5M_{\odot}$ reference model. As a consequence, a smaller expansion ensues and a stable laminar flame propagating to the center can develop. A close inspection of the energetics in the vicinity of the flame indicates that most of the nuclear energy production is generated in the so-called “precursor flame”, consisting of a thin radiative zone of a few kilometers width located just below the so-called convective flame. In the precursor flame, the nuclear energy production is maximum, the neutrino energy loss rate is weak and the luminosity is negative. Thus, the energy flows inward and is actually used to expand and heat the inner layers. Just like a deflagration, this energy flux pre-heats the material ahead of the flame front and when the matter has been nuclearly processed, convection moves inward and absorbs the nuclear ashes. Inside the convective flame a steady state is achieved where the luminosity at the base and at the top of the flame, i.e. the energy flowing into and out of the convective zone, are almost equals. In other words, there is an almost perfect balance between the loss of energy by neutrinos and the energy produced by nuclear burning and released by the

contraction of the structure (see Timmes *et al.*

1994, for a detailed analysis of carbon deflagration). The velocity of the flame front is typically of the order of 10^{-3}cm s^{-1} and is highly subsonic since in this region the sound speed is $> 2 \times 10^8 \text{cm s}^{-1}$. When the flame reaches the center (after 11700 yr in our reference model), convection disappears and carbon burning proceeds in a shell. Eventually, short-lived secondary convective instabilities can develop at the re-ignition of some carbon pockets (Fig. 2).

With increasing initial stellar mass, the mass coordinate of carbon ignition gets closer to the center as the degeneracy of the central region decreases. Ultimately, for stars massive enough, carbon ignites directly at the center. We also report that the strength of the carbon flash decreases as the initial mass increases (see Siess 2006a, for more details).

Carbon burning is powered by $^{12}\text{C}(^{12}\text{C},\alpha)^{20}\text{Ne}$ and $^{12}\text{C}(^{12}\text{C},\text{p})^{23}\text{Na}$ reactions followed in third place by $^{16}\text{O}(\alpha,\gamma)^{20}\text{Ne}$. These reactions convert the CO core into a NeO mixture and supply protons and α particles for a richer nucleosynthesis. In particular, the α particles that do not react with ^{16}O contribute to the complete destruction of ^{22}Ne (formed during core He burning) by (α,n) and (α,γ) reactions, thus leading to the production of ^{25}Mg and ^{26}Mg . The protons mainly react with ^{23}Na and via the (p,α) and (p,γ) channel increase the mass fraction of ^{20}Ne and ^{24}Mg , respectively. They also participate to the production of ^{27}Al by (p,γ) reactions on ^{26}Mg . At the end of the carbon burning phase, the core is mainly composed (by mass) of ^{16}O (55-60%) and ^{20}Ne (29-32%) with some traces of ^{23}Na (5-6%) and ^{24}Mg (3%).

2.2. The second dredge-up

Following the formation of the NeO core, the central regions contract again and the release of gravothermal energy produces an expansion of the structure which induces the deepening of the convective envelope during the so-called second-dredge-up (2DUP). Depending of the initial stellar mass, the 2DUP can take place before carbon ignition (as in AGB stars), during the main carbon burning phase or not

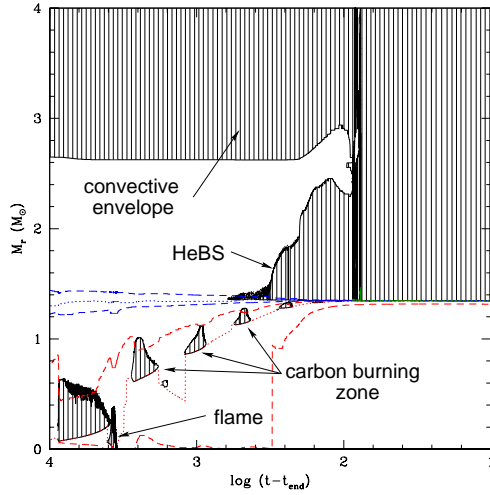


Fig. 3. “Dredge-out” phenomenon at the end of core carbon burning in a $Z = Z_{\odot}$ $10.8M_{\odot}$.

at all as in massive stars. Contrarily to AGB stars, after crossing the HBS the envelope of SAGB stars reaches the top of the (extinct) He burning shell (HeBS). The surface composition then shows a substantial increase in ${}^4\text{He}$ and ${}^{12}\text{C}$ and of course of the product of H-burning (mainly ${}^{14}\text{N}$ and ${}^{13}\text{C}$). However, in the most massive SAGB stars a new phenomenon, the so-called dredge-out phenomenon (Iben *et al.* 1997) takes places. In this process (Fig. 3), a convective zone develops in the HeBS, grows in mass and merges with the envelope. An important consequence of this phenomenon is a significant decrease in the H-depleted core (by $\gtrsim 1M_{\odot}$), that can play a critical role in the final fate of these stars (see Siess & Pumo 2006, for details).

3. Mass transitions

SAGBs are at the cross road of stellar evolution. As outlined in the introduction, stars in this mass range can have very different fates depending on their initial mass and on the adopted mass loss rate prescription. The first mass transition, usually referred to as M_{up} , corresponds the minimum initial stellar mass for carbon ignition. However it must be emphasized that M_{up} critically depends on the

adopted treatment of mixing at the edge of the He-core. For instance, Bertelli *et al.* (1985) showed that for solar metallicity models, core overshooting during He-burning decreases the value of M_{up} from 9 to $6M_{\odot}$! The second mass transition, M_{n} corresponds to the minimum initial stellar mass for a SAGB star to evolve into an electron-capture supernova. In the 80’s Nomoto (1984) showed that if the NeO core mass exceeds a critical value of $M_{\text{EC}} \sim 1.37M_{\odot}$, then electron captures come into play leading to core collapse and supernova explosion. M_{n} thus defines the initial stellar mass for which, by the end of the evolution, the NeO core mass has reached M_{EC} . It also defines the minimum mass for the formation of a neutron star. In practice, to determine this number, we take the NeO core mass at the end of carbon burning. Then, assuming a constant core growth rate of $\dot{M}_{\text{core}} = 5 \times 10^{-7}M_{\odot} \text{ yr}^{-1}$, we considered 2 extreme cases of a constant mass loss rate equals to $\dot{M}_1 = 3 \times 10^{-5}M_{\odot} \text{ yr}^{-1}$ and $\dot{M}_2 = 10^{-4}M_{\odot} \text{ yr}^{-1}$. Under these assumptions, we can derive analytically the final mass of the NeO core when the envelope is removed. If this value is larger than M_{EC} , then EC-SN will ensue. Finally, the third mass transition M_{SN} represents the initial mass above which the evolution proceeds through all the nuclear burning stages and leads to a type II supernova. Following Nomoto (1984) stars that have a NeO core mass larger than M_{EC} at the end of carbon burning will follow this evolutionary path.

Our study is based on the computation of a large grid of 74 stellar models covering a mass range between 7 and $13M_{\odot}$ and for 5 different metallicities (Z) between 10^{-5} and 0.04 (Siess & Pumo 2006). When varying Z , the hydrogen and helium mass fractions are given by $X = X_{\text{BB}} + (X_{\odot} - X_{\text{BB}})Z/Z_{\odot}$ and $Y = 1 - X - Z$, where the solar and primordial hydrogen values equal $X_{\odot} = 0.710847$ and $X_{\text{BB}} = 0.7521$ (Coc *et al.* 2004), respectively. The mass fraction of metals is scaled from the solar distribution of Grevesse *et al.* (1996).

The results are depicted in Fig. 4 which shows the behavior of the different mass transitions as a function of initial composition. As the metallicity decreases, both M_{up} and M_{SN}

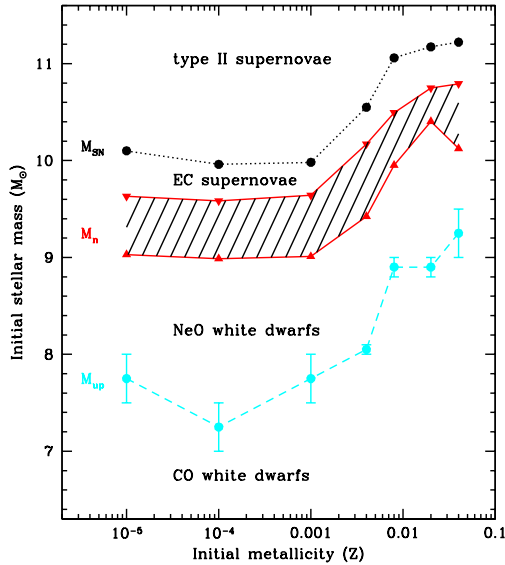


Fig. 4. Mass transitions as a function of initial metallicity. The lower and upper boundaries for M_n are computed assuming a constant mass loss rate of $3 \times 10^{-5} M_\odot \text{ yr}^{-1}$ and $10^{-4} M_\odot \text{ yr}^{-1}$, respectively.

decrease. This is easily explained by the fact that, when the metal content decreases, the opacity drops. Stars are thus more luminous and develop larger cores to balance the energy leak from the surface. However at very low metallicity ($Z \lesssim 10^{-4}$), this opacity dependence on metal is weaker (Cassisi & Castellani 1993) and the trend is reversed. Our analysis also reveals that the value of M_n is very dependent on the mass loss rate and in all cases, is restricted to a very narrow mass range, of less than $\sim 1 M_\odot$. It should be pointed out that the value of M_n also depends on the presence or not of third dredges-up (3DUP) which affects the core growth rate (Poelarends et al. in this volume). This figure also shows that the initial mass range for the formation of NeO white dwarf is relatively small ($1-1.5 M_\odot$) and that it used to be larger in the past, at lower metallicity. Finally, let us stress again that these mass transitions critically depend on the treatment of mixing, in particular during core He burning. Additional models (not shown) including core overshooting at the edge of the He core (with $f_{\text{over}} = 0.016$ as described in Goriely & Siess

2004) show that all the mass transitions are all shifted downward by $\sim 2 M_\odot$.

4. The TP-SAGB phase

Stars with initial mass between M_{up} and M_{SN} will enter the thermally pulsing SAGB phase after the extinction of carbon burning. Like their lower mass counterpart, the He burning shell suffers recurrent instabilities but the properties are significantly different. First, the He luminosity generated during the pulse is much weaker in SAGB compared to standard AGB stars by one or two orders of magnitude. The reason is mainly attributed to the larger contribution of the radiation pressure to the total pressure and to the weaker degeneracy in SAGB stars which both lead to a quicker response of the structure ($P_{\text{rad}} \propto T^4$) to a temperature increase and thus to a more rapid quenching of the thermal pulse (Siess 2006b). The evolution during the AGB phase is primarily governed by the core mass (M_c) and as M_c increases the interpulse and pulse duration shorten. Quantitatively, we find that for a 10 and $10.5 M_\odot$ ($Z = Z_\odot$) model, the interpulse duration is of the order of 200 and 20 yr, respectively. This is much shorter than in standard AGB stars where typical values for a $5 M_\odot$ model are of the order of a few thousand years. The duration of the thermal pulse is also considerably reduced in SAGB stars, ~ 1 yr in a $10 M_\odot$ and 0.2 yr in a $10.5 M_\odot$, compared to 10-20 yr in a $5 M_\odot$. With these numbers, one can expect SAGB stars to suffer 300 to 1000 thermal pulses, a nightmare for modelers! Finally, let us note that the mass of the convective pulse is very small, less than $\sim 10^{-4} M_\odot$ which might strongly limit the role of SAGB stars in the chemical evolution.

The question of the 3DUP is a matter of strong debate among AGB stars modelers. Our models, which do not include any extra-mixing and use the Schwarzschild criterion to delineate the convective boundaries, do not experience 3DUP, as also found by Ritossa *et al.* (1996), Poelarends et al. (this volume) but contrary to Doherty & Lattanzio (this volume) who find deep 3DUPs with λ as high as 0.7. In our case, this is not surprising considering

the weakness of the pulse, the absence of extra-mixing and the fact that the HBS remains active at all times.

Concerning the nucleosynthesis, owing to their large core mass and strong gravity, the temperature at the base of the thermal pulse is high and can easily exceed 3.4×10^8 K. Under these circumstances, the $^{22}\text{Ne}(\alpha, n)^{25}\text{Mg}$ neutron source can be efficiently activated. The possibility of s-process nucleosynthesis in the pulse of SAGB is a priori favored but the short duration of the instability (< 1 yr) might lead to neutron exposures too small for an effective s-process. The temperature at the base of the envelope is also relatively high in SAGB stars and hot bottom burning (HBB) takes places. This leads to the activation of the NeNa and MgAl cycles and therefore to the production of ^{23}Na , Mg isotopes and ^{27}Al . However, for these chains to be efficient, very high temperatures are required at the base of the convective envelope. In our models the temperature remains moderate $T_{\text{env}} \simeq 6 - 8 \times 10^7$ K and these chains are partially activated. However, Doherty & Lattanzio and Poelarends et al. (this volume) using different codes find very high temperatures, largely above 10^8 K.

5. Discussion

Our current knowledge of the evolution of thermally pulsing SAGB is very sparse and from the presentations given at this meeting, the results show large discrepancies. Some models develop very deep dredges up while others none, some exhibit very high temperatures at the base of the convective envelope while other only moderate temperatures. These evolution features affect the stars when stellar winds are strong and thus when the star contributes the most to the chemical evolution of the galaxy. Despite these differences some conclusions can however be drawn. First, the occurrence or not of the 3DUP, will not affect substantially the surface composition. This is mainly the result of the huge envelope mass ($\sim 8-10M_{\odot}$) compared to the tiny pulse mass

(at most a few $10^{-4}M_{\odot}$). The dilution factors are so large that 3DUP pollution will have almost no effect on the surface abundances, at least as long as the metallicity is not “too low”. However, as pointed out in §3, the 3DUPs modify the core growth rate and thus can affect the fate of the star and incidentally its yields.

Concerning HBB, its effect may be not as large as expected for two reasons: first, there is a large amount of matter to process (the entire envelope) and second the life time on the SAGB is rather small ($\sim 10^5$ yr). So given this short duration, substantial modifications of the envelope composition will require very high temperatures at its base. As far as the yields are concerned, this latter quantity is certainly of uttermost importance.

Acknowledgements. LS is FNRS research associate.

References

- Bertelli, G., Bressan, A.G., & Chiosi, C. 1985, *A&A*, 150, 33
- Cassisi S., Castellani V. 1993, *ApJS*, 88, 509
- Coc A., Vangioni-Flam E., Descouvemont P. *et al.* 2004, *ApJ*, 600, 544
- Goriely S., Siess L. 2004, *A&A*, 421, L25
- Grevesse N., Noels A., Sauval A.J. 1996, *ASPC*, 99, 117
- Iben I., Ritossa C., Garcia-Berro E. 1997, *ApJ*, 489, 772
- Nomoto K. 1984, *ApJ*, 277, 791
- Ritossa C., Garcia-Berro E., Iben I. 1996, *ApJ*, 460, 489
- Siess L. 2006a, *A&A*, 448, 707
- Siess L. 2006b, “Stars and Nuclei: A Tribute to Manuel Forestini”, *EAS Publication Series*, in press
- Siess L., Pumo M.L. 2006, *A&A*, in preparation
- Straniero O., Chieffi A., Limongi M. *et al.* 1997, *ApJ*, 478, 332
- Timmes F.X., Woosley S.E., Taam R.E. 1994, *ApJ*, 420, 348